

# Lawrence Berkeley National Laboratory

## LBL Publications

### Title

Doped Nanocrystals as Plasmonic Probes of Redox Chemistry

### Permalink

<https://escholarship.org/uc/item/2ns1w9p7>

### Journal

Angewandte Chemie International Edition, 52(51)

### ISSN

14337851

### Authors

Jain, Prashant K.  
Manthiram, Karthish  
Engel, Jesse H.  
[et al.](#)

### Publication Date

2013-10-23

# Doped Nanocrystals as Plasmonic Probes of Redox Chemistry\*\*

Prashant K. Jain,\* Karthish Manthiram, Jesse H. Engel, Sarah L. White, Jacob A. Faucheaux, and A. Paul Alivisatos\*

The use of nanostructured probes for chemical sensing has opened up the ability to detect ultra-low analyte volumes and achieve nanoscale spatial resolution. Metal nanoparticles exhibiting localized surface plasmon resonances (LSPRs) have been at the forefront of this research<sup>[1–5]</sup> for two reasons: 1) LSPR scattering can be routinely measured from single nanoparticle probes and 2) the frequency of the LSPR band is highly sensitive to the local refractive index ( $n_m$ ) around the nanoparticle as per the resonance condition:<sup>[6,7]</sup>

$$\varepsilon_r(\omega) = -2n_m^2 \quad (1)$$

where  $\varepsilon_r$  is the real part of the metal dielectric function as a function of optical frequency  $\omega$ . Analytes, which induce a change in the local refractive index around the nanoparticle, are detected by shifts in the frequency of the LSPR scattering band. The method, while powerful, is limited: chemical events, which do not involve a large enough change in refractive index, go undetected.

Herein, we describe LSPRs of doped semiconductor nanocrystals that are sensitive to redox processes and surface chemistry. We take advantage of the fact that the LSPR frequency is proportional to the square root of the carrier concentration within the nanocrystal. We show, using a few different examples, that chemical events occurring locally on the nanocrystal can cause a change in the doping level and carrier concentration within the nanocrystal, resulting in large shifts in the LSPR. The basis of this sensitivity is therefore truly chemical, rather than refractive-index mediated, unlike conventional metal-nanoparticle-based plasmonic probes.

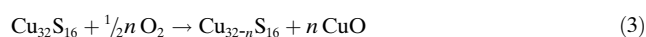
We employ nanorods of the semiconductor copper(I) sulfide, which the Alivisatos and Burda groups have shown to

exhibit near-infrared LSPRs owing to heavy *p*-doping resulting from a high level of copper vacancies.<sup>[8,9]</sup> Others have shown similar LSPRs in nanocrystals of copper(I) selenide and copper(I) telluride.<sup>[10–16]</sup> LSPR tunability by variation of the copper vacancy concentration has also been demonstrated by the Alivisatos and Manna groups: the greater the vacancy concentration, the higher the LSPR frequency.<sup>[9,10]</sup> Metal nanoparticles do not possess such tunability, as their free carrier concentrations are large and difficult to perturb appreciably.

We exploit the well-known chemical sensitivity of copper(I) sulfide,<sup>[17]</sup> which can be summarized by the chemical reaction:<sup>[18]</sup>



The creation of one Cu vacancy per unit cell ( $n = 1$ ) results in copper-deficient sulfide (with a unit cell of  $\text{Cu}_{31}\text{S}_{16}$ ), which is thermodynamically more stable, by  $-7.3$  eV, than the fully stoichiometric form (with a unit cell of  $\text{Cu}_{32}\text{S}_{16}$ ). The reaction direction is, however, dictated by the chemical potential of Cu ( $\mu_{\text{Cu}}$ ) in the additional copper species formed on the right. In general, conditions which stabilize copper (such as lower  $\mu_{\text{Cu}}$ ) favor the forward reaction involving the formation of copper vacancies and valence band holes. For example, copper is much more stable in the form of copper oxide than as  $\text{Cu}^0$ ; therefore, the creation of copper vacancies is strongly favored (Scheme 1 a) in the presence of air or other oxidants:<sup>[9]</sup>



[\*] Prof. P. K. Jain, S. L. White, J. A. Faucheaux  
Department of Chemistry, University of Illinois at Urbana  
Champaign, 600 S. Mathews Ave, Urbana, IL 61801 (USA)  
E-mail: jain@illinois.edu  
Homepage: <http://www.nanogold.org>

Prof. P. K. Jain  
Department of Physics and Materials Research Lab, University of  
Illinois at Urbana Champaign, Urbana, IL 61801 (USA)

K. Manthiram, J. H. Engel, Prof. A. P. Alivisatos  
Materials Sciences Division, Lawrence Berkeley National Laboratory  
Berkeley CA 94720 (USA)  
E-mail: apalivisatos@lbl.gov  
Homepage: <http://www.cchem.berkeley.edu/pagrp/>

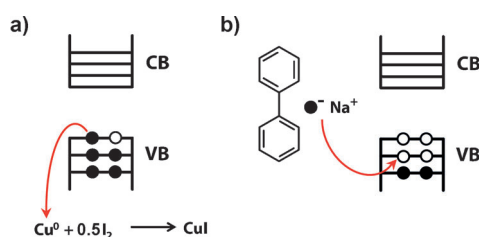
K. Manthiram  
Department of Chemical and Biomolecular Engineering, University  
of California at Berkeley, Berkeley, CA 94720 (USA)

J. H. Engel, Prof. A. P. Alivisatos  
Department of Materials Science, University of California at  
Berkeley, Berkeley, CA 94720 (USA)

[\*\*] Work by P.K.J. and S.L.W. on oxidation/reduction chemistry of  
nanocrystals and their plasmonic/structural characterization was  
supported by the Dupont Young Professor Award (P.K.J.). Simu-  
lations were supported by a National Science Foundation Graduate  
Research Fellowship awarded to J.F. under Grant No. DGE-1144245  
and an IACAT fellowship to P.K.J. Work on methods of nanocrystal  
doping was supported by the Physical Chemistry of Inorganic  
Nanostructures Program, KC3103, Director, Office of Science,  
Office of Basic Energy Sciences, of the United States Department of  
Energy under contract DE-AC02-05CH11231 and a graduate fel-  
lowship awarded to K.M. from the Department of Energy Office of  
Science Graduate Fellowship Program (DOE SCGF), made possible  
in part by the American Recovery and Reinvestment Act of 2009,  
administered by ORISE-ORAU under contract no. DE-AC05-  
06OR23100. Electrical characterization by J.H.E. was supported by  
Self-Assembly of Organic/Inorganic Nanocomposite Materials  
(Grant DE-AC02-05CH11231 to A.P.A.). We thank Jessy Rivest for  
CdS nanorod samples.



Supporting information for this article is available on the WWW  
under <http://dx.doi.org/10.1002/anie.201303707>.



**Scheme 1.** Chemical sensitivity of copper(I) sulfide. a) The presence of oxidants such as iodine favors the creation of copper vacancies, resulting in holes in the valence band of copper(I) sulfide. b) The presence of electron donors such as sodium biphenyl results in filling of the copper vacancies.

Along with  $\text{CuO}$ ,<sup>[12]</sup>  $\text{Cu}_2\text{O}$ , known to be stable on the nanoscale,<sup>[19]</sup> may also be formed. Reducing conditions, on the other hand, favor the backward reaction involving the filling of copper vacancies (Scheme 1b). Owing to the high diffusivity of copper atoms in copper(I) sulfide, a well-known solid-state ionic material,<sup>[20]</sup> reaction kinetics do not appear to be a limiting factor, especially in nanocrystals.

In particular, we show that ligands such as alkylamines and oxidants such as iodine cause *p*-doping of the copper sulfide nanorods, manifested by strengthening and blue-shift of the LSPR band. On the other hand, ligands such as thiols and electron donating reagents such as sodium biphenyl reduce the *p*-doping level of the nanorods, resulting in a red-shift and suppression of the LSPR. By means of electrical measurements, we corroborate that shifts in carrier concentrations are indeed the cause of the observed LSPR changes. The *p*-type conductivity of copper(I) sulfide nanorod films is enhanced under oxidizing conditions. The application of reducing conditions causes a reversal of the conductivity increase. Our results suggest that doped semiconductor nanocrystals can be used for plasmonic detection of chemical events, such as charge transfer, redox chemistry, doping, and ligand binding. In particular, the ability of common ligands such as amines and thiols to electronically dope quantum dots is verified by taking advantage of the optical and electrical sensitivity of the copper(I) sulfide system. We also provide a detailed characterization of the chemical changes that accompany redox chemistry and the doping of nanocrystals.

Copper(I) sulfide nanorods used for the studies here were obtained by cation exchange of cadmium sulfide nanorods with excess  $\text{Cu}^+$  (see the Supporting Information), a method known to yield nanorods with a negligible number of copper vacancies,<sup>[9]</sup> as evidenced by the low electrical conductivity of the nanorods and the lack of plasmonic absorption in the near-infrared region.

The equilibrium copper vacancy density and *p*-type doping of copper sulfide nanorods can be increased by the addition of ligands or oxidants. We hypothesized that the addition of amines, which bind strongly to copper, should assist in extracting copper from the copper sulfide lattice, thus pushing the equilibrium indicated in Equation [2] to the right. More copper-deficient stoichiometries ( $\text{Cu}_{30}\text{S}_{16}$ ,  $\text{Cu}_{29}\text{S}_{16}$ , and so on) are also possible.<sup>[21]</sup> Upon addition of amine to stoichiometric copper sulfide nanocrystals, we observed that a strong LSPR mode appeared. Copper appears to be

removed from the lattice by way of formation of a copper-amine complex, detected by its absorption band at ca. 680 nm (Figure S3b). The LSPR mode blue-shifted and increased in intensity upon each subsequent addition of decylamine (Figure 1a), thus demonstrating the utility of using LSPR to monitor progressive changes in the carrier density.

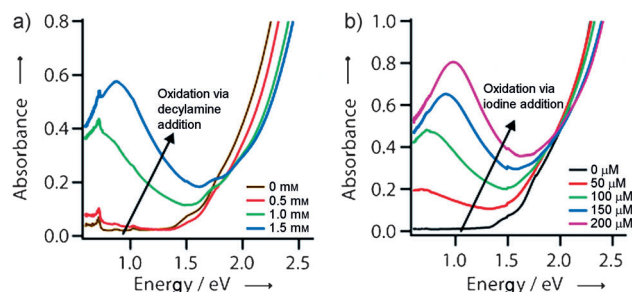


**Figure 1.** LSPR detection of vacancies formed in copper(I) sulfide nanorods by means of ligands or common oxidants. Addition of decylamine (a) or iodine (b) to fully stoichiometric copper sulfide nanorods results in the emergence of an LSPR mode due to the formation of copper vacancies and associated hole carriers. With increasing addition of amine or iodine, the vacancy concentration increases, as manifested by a progressive blue-shift and increase in intensity of the LSPR band. The band-gap absorption onset and excitonic peak also blue-shift, as expected from an increase in free carrier concentration (Moss–Burstein shift). The starting nanorods were prepared by the cation exchange of  $\text{CdS}$  with  $\text{Cu}^+$  salt under air-free conditions, a method which yields fully stoichiometric or vacancy-free  $\text{Cu}_2\text{S}$ .

Given that copper extraction from copper sulfide is an oxidative process, we also hypothesized that common oxidants such as iodine should be capable of the oxidative extraction of copper ions from copper sulfide through the formation of copper iodide:

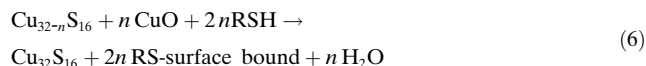
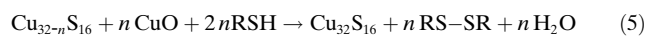


The addition of iodine to copper sulfide nanorods led to the emergence of an LSPR mode, which gradually blue-shifted and increased in intensity upon incremental iodine additions (Figure 1b). The ca. 1 eV peak position of the LSPR mode achieved by the addition of 200  $\mu\text{M}$  iodine corresponds to a stoichiometry of  $\text{Cu}_{29}\text{S}_{16}$  or  $\text{Cu}_{1.8}\text{S}$  (see the Supporting Information), known to be the digenite phase. Concomitant with copper extraction, copper iodide was formed, as verified by the appearance of its characteristic absorption band at 410 nm (Supporting Information, Figure S3a).

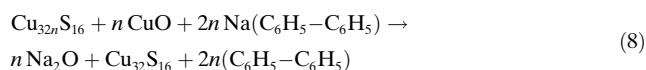
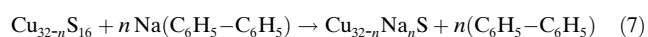
Thus, both oxidative and non-oxidative copper extraction can be detected by blue-shifts in the LSPR band. Upon copper extraction, the band-edge absorption also blue-shifts, known as a Moss–Burstein shift, as expected from an increase in the free carrier concentration within the nanocrystals.<sup>[9]</sup>

Just as the equilibrium of Equation [2] can be driven to the right by the addition of ligands or oxidants, we expected that the equilibrium could also be shifted to the left by the addition of reducing agents. Thiols are known to be mild reducing agents; incremental addition of undecanethiol to air-

oxidized copper(I) sulfide nanorods drove the filling of copper vacancies, as evidenced by a gradual shift in the LSPR to lower energies and a reduction in the intensity of the mode. A possible mechanism can involve either disulfide formation or coordination of the thiol to metal atoms on the nanocrystal surface:



Similarly, the addition of strong reducing agents such as sodium biphenyl (Figure 2b) also resulted in a red-shift and suppression of the LSPR band. Sodium biphenyl has been shown to inject electrons into nanocrystals,<sup>[22]</sup> which serves to reverse the hole vacancies in the lattice (Scheme 1b), although it is unclear as to whether the vacancy is filled by a sodium ion or a copper ion.<sup>[23]</sup>



The absorption band-edge also shifted to lower energies upon addition of either reducing agent, as expected from a decrease in the carrier concentration within the nanocrystals. Complete reversal to  $\text{Cu}_2\text{S}$  did not appear possible (Figure 2a), at least with the mildly reducing thiol. Near-complete suppression of the LSPR was, however, observed (Figure S4) with the stronger reducing ability of sodium biphenyl and another reagent, cobaltocene, probably when

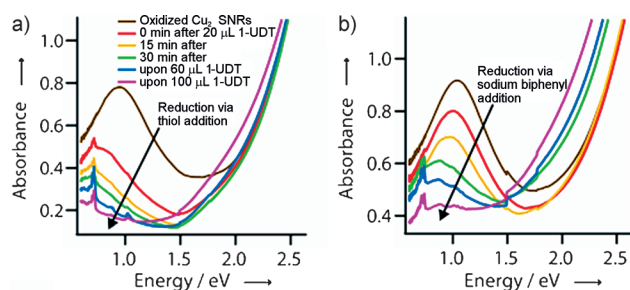


**Figure 2.** LSPR detection of vacancy filling in copper(I) sulfide nanorods by reduction with thiol (a) or electron injection with sodium biphenyl (b). The addition of undecanethiol (a) or sodium biphenyl (b) to a solution of copper(I) sulfide nanorods results in a progressive red-shift of the LSPR mode and a reduction in its intensity. A concomitant red-shift of the band-edge absorption onset is also seen. These effects are a manifestation of the progressive filling of vacancies in the nanorod lattice, owing to the reducing ability of the thiol or the electron-injecting ability of sodium biphenyl. Features around 0.72 eV, 0.87 eV, and 1.0 eV are due to ligand/thiol vibrational absorption. The sharp step at 1.5 eV is an instrumental artifact from a spectrophotometer grating change. Copper-deficient copper(I) sulfide nanorods were prepared by oxidation of fully stoichiometric  $\text{Cu}_2\text{S}$  nanorods in air. Reduction experiments were carried out in an air-free environment in tetrachloroethylene or carbon tetrachloride, which are solvents with low near-infrared absorbance. The concentration of undecanethiol or sodium biphenyl added to achieve complete reversal was ca. 100 mM.

employed in excess.<sup>[24]</sup> Copper oxide or copper iodide could present a physical barrier, in the form of a thick shell over the nanorod, or a chemical barrier against complete vacancy filling. Also, copper oxide and iodide are *p*-type semiconductors, whose electronic properties can complicate plasmonic spectra of the nanorods. But, the influence of a copper oxide or iodide shell on the NIR LSPR of the nanorods is estimated to be a small nonresonant dielectric effect, as both these semiconductors have band-to-band transitions in the visible region (Figure S5). Also, the hole-density of either *p*-type semiconductor is not adequate to support an NIR intraband absorption or LSPR of its own.

Electrical measurements serve to directly confirm that the chemical events responsible for LSPR changes indeed modulate the doping level and carrier concentration within the nanocrystal.<sup>[25]</sup> The conductivity of a nanocrystal film scales monotonically with the free carrier concentration of the effective media:

$$\sigma = N e \mu \quad (9)$$

where  $N$  is the majority free carrier density,  $e$  is the elemental charge, and  $\mu$  is the free carrier mobility. Equation (9) assumes ohmic conduction and carrier-concentration-independent mobility, which are reasonable approximations for a heavily doped transistor device.<sup>[26]</sup> Moreover, regardless of the assumptions, conductivity still varies monotonically with the free carrier concentration.

We investigated the effects of redox doping on the electrical properties of nanorod films through field-effect transistor (FET) measurements. Films of freshly exchanged copper(I) sulfide nanorods were drop-cast from solution onto highly doped silicon substrates with 300 nm of thermally grown gate oxide and patterned gold contacts. Film thicknesses were estimated at ca.  $150 \pm 50$  nm from profilometry. After drop-casting, films were initially soaked in a solution of ethanethiol (EtSH; 1 mM) in ethanol to permit exchange with the native long-chain oleic acid or phosphonic acid ligands, decrease interparticle spacing, and increase conductivity.<sup>[27]</sup> As is typical for heavy doping, the films exhibited large linear conductivity and no transconductance modulation with applied gate voltage, thus prohibiting the extraction of field-effect mobilities (see the Supporting Information).

As shown in Figure 3a, the small-field (10 mV source-drain) conductivity of the initial film increases dramatically upon exposure to air, rising over two orders of magnitude over 40 h as oxygen creates copper vacancies within the nanocrystals (Eq. [3]). Figure 3b demonstrates a complete reversal of this trend upon soaking of the film in an ethanolic solution of EtSH (1 mM), a reducing agent. These oxidation and reduction steps are shown to be reversible and repeatable (Figure 3c), exhibiting near identical response upon consecutive treatments. In nanoparticle films treated with thiols, oxidation can often lead to a lowering of effective mobility as surface oxides can increase quantum confinement and edge-edge hopping distances.<sup>[26]</sup> While it is unfeasible to deconvolute changes in mobility and carrier concentration for these heavily doped films, the changes in conductivity likely represent a lower bound for the relative changes in doping

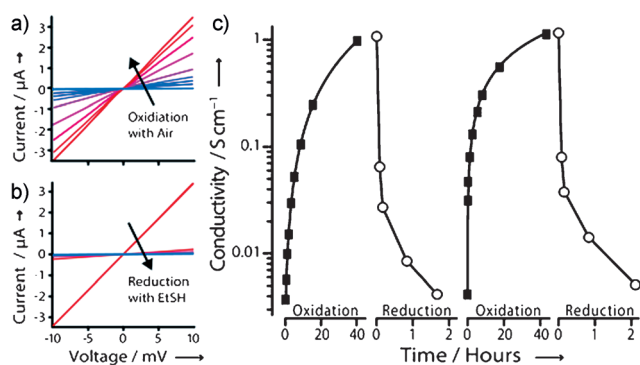


**Figure 3.** Reversible formation and filling of vacancies in copper(I) sulfide nanorod films probed electrically. The small-field conductivity of copper(I) sulfide nanorod thin-film FETs increases over two orders of magnitude upon exposure to air (a) and completely reverses upon soaking in a solution of ethanethiol (EtSH; 1 mM) in ethanol (b). Conductivity measurements on a single device (c) demonstrate reversible vacancy-formation and filling by sequential oxidation and reduction steps. For the measurements, the films were initially soaked in an EtSH solution to displace long-chain ligands and boost inter-particle conductivity. The oxidation steps were performed in air with continuous measurement on an open-air probe station. The reduction steps were performed in an argon glovebox. Conductance was measured between patterned gold contacts with channel lengths of 10  $\mu\text{m}$  and widths of 250  $\mu\text{m}$ .

level. If the redox processes do introduce changes in effective mobility, they also must be reversible, as Figure 3c shows the conductivity to be sequentially reversible on the same device. Irreversible chemical changes likely do not play a large role in these treatments, demonstrating the thermodynamic nature of copper vacancy formation and reversal.

A doped semiconductor nanocrystal may potentially be used to achieve plasmonic detection of a single molecule or a single chemical event. This is possible by using a nanocrystal of small-enough size. For example, in a 4 nm nanocrystal, which has a volume of 34  $\text{nm}^3$ , the creation of a single copper vacancy is equivalent to an increase ( $dN$ ) of  $3 \times 10^{19} \text{ cm}^3$  in the carrier concentration. For a nominally copper-deficient nanocrystal with a carrier concentration ( $N$ ) of  $1.5 \times 10^{21} \text{ cm}^3$ , this is equivalent to a 2% increase in carrier concentration. As the LSPR wavelength is related to carrier concentration:<sup>[7]</sup>

$$\lambda_{\text{sp}} \propto \frac{1}{\sqrt{N}} \quad (10)$$

we have:

$$\frac{d\lambda_{\text{sp}}}{\lambda_{\text{sp}}} \propto -\frac{dN}{2N} \quad (11)$$

Thus, the formation of a single copper vacancy would result in a blue-shift in the LSPR wavelength by 1%, which is about 15–20 nm in the 2  $\mu\text{m}$  spectral region. Such shifts can be measured without difficulty, allowing quantized events to be detected on a nanocrystal. Whereas the acquisition of single-particle LSPR scattering spectra in the near-infrared remains a challenge, the approach is feasible, in principle.

In summary, our work demonstrates qualitatively the ability to use semiconductor nanocrystals for plasmonic probing of processes, such as redox reactions, electrochemical charging or discharging, ligand binding, and impurity doping, occurring in nanoscale volumes. In the past, such probing has been carried out by means of electrical detection on nanostructures.<sup>[28]</sup> But, optical probing through plasmon scattering opens up the possibility of remote detection. Physical contact with the nanostructure will not be required, rendering detection non-perturbative. High throughput could be achieved by simultaneous addressing of several individual nanocrystals. Detection of single-molecule events also seems feasible by use of small nanocrystals. Given the promise, there is a need to explore a wider range of chemical and redox processes beyond the limited examples we have provided in the current work.

Received: April 30, 2013

Published online: October 23, 2013

**Keywords:** copper sulfide · doping · ion exchange · nanocrystals · semiconductor plasmons

- [1] Y. Sun, Y. Xia, *Anal. Chem.* **2002**, *74*, 5297–5305.
- [2] A. D. McFarland, R. P. Van Duyne, *Nano Lett.* **2003**, *3*, 1057–1062.
- [3] F. Tam, C. Moran, N. J. Halas, *J. Phys. Chem. B* **2004**, *108*, 17290–17294.
- [4] K. A. Willets, R. P. Van Duyne, *Annu. Rev. Phys. Chem.* **2007**, *58*, 267–297.
- [5] B. Yan, S. V. Boriskina, B. M. Reinhard, *J. Phys. Chem. C* **2011**, *115*, 24437–24453.
- [6] S. Underwood, P. Mulvaney, *Langmuir* **1994**, *10*, 3427–3430.
- [7] P. K. Jain, M. A. El-Sayed, *J. Phys. Chem. C* **2007**, *111*, 17451–17454.
- [8] Y. Zhao, H. Pan, Y. Lou, X. Qiu, J. Zhu, C. Burda, *J. Am. Chem. Soc.* **2009**, *131*, 4253–4261.
- [9] J. M. Luther, P. K. Jain, T. E. Ewers, A. P. Alivisatos, *Nat. Mater.* **2011**, *10*, 361–366.
- [10] J. Choi, N. Kang, H. Y. Yang, H. J. Kim, S. U. Son, *Chem. Mater.* **2010**, *22*, 3586–3588.
- [11] C. M. Hessel, V. P. Pattani, M. Rasch, M. G. Panthani, B. Koo, J. W. Tunnell, B. A. Korgel, *Nano Lett.* **2011**, *11*, 2560–2566.
- [12] D. Dorfs, T. Härtling, K. Miszta, N. C. Bigall, M. R. Kim, A. Genovese, A. Falqui, M. Povia, L. Manna, *J. Am. Chem. Soc.* **2011**, *133*, 11175–11180.
- [13] F. Scotognella, G. D. Valle, A. R. S. Kandada, D. Dorfs, M. Zavelani-Rossi, M. Conforti, K. Miszta, A. Comin, K. Korobchevskaya, G. Lanzani, L. Manna, F. Tassone, *Nano Lett.* **2011**, *11*, 4711–4717.
- [14] A. L. Routzahn, S. L. White, L.-K. Fong, P. K. Jain, *Isr. J. Chem.* **2012**, *52*, 983–991.
- [15] I. Kriegel, C. Jiang, J. Rodríguez-Fernández, R. D. Schaller, D. V. Talapin, E. da Como, J. Feldmann, *J. Am. Chem. Soc.* **2012**, *134*, 1583–1590.
- [16] I. Kriegel, J. Rodríguez-Fernández, A. Wisnet, H. Zhang, C. Waurisch, A. Eychmüller, A. Dubavik, A. O. Govorov, J. Feldmann, *ACS Nano* **2013**, *7*, 4367–4377.
- [17] M. Lotfipour, T. Machani, D. P. Rossi, K. E. Plass, *Chem. Mater.* **2011**, *23*, 3032–3038.
- [18] P. Lukashev, W. R. L. Lambrecht, T. Kotani, M. van Schilf-gaarde, *Phys. Rev. B* **2007**, *76*, 195202.



- [19] M. Yin, C.-K. Wu, Y. Lou, C. Burda, J. T. Koberstein, Y. Zhu, S. O'Brien, *J. Am. Chem. Soc.* **2005**, *127*, 9506–9511.
- [20] P. Knauth, H. L. Tuller, *J. Am. Ceram. Soc.* **2002**, *85*, 1654–1680.
- [21] A. Putnis, *Am. Mineral.* **1977**, *62*, 107–114.
- [22] M. Shim, P. Guyot-Sionnest, *Nature* **2000**, *407*, 981–983.
- [23] J. S. Kim, D.-Y. Kim, G.-B. Cho, T.-H. Nam, K.-W. Kim, H.-S. Ryu, J.-H. Ahn, H. J. Ahn, *J. Power Sources* **2009**, *189*, 864–868.
- [24] W.-k. Koh, A. Y. Kopoulos, J. T. Stewart, B. N. Pal, I. Robel, J. M. Pietryga, V. I. Klimov, *Sci. Rep.* **2013**, *3*, 2004.
- [25] E. J. D. Klem, H. Shukla, S. Hinds, D. D. MacNeil, L. Levina, E. H. Sargent, *Appl. Phys. Lett.* **2008**, *92*, 212105.
- [26] M. H. Zarghami, Y. Liu, M. Gibbs, E. Gebremichael, C. Webster, M. Law, *ACS Nano* **2010**, *4*, 2475–2485.
- [27] J. M. Luther, M. Law, Q. Song, C. L. Perkins, M. C. Beard, A. J. Nozik, *ACS Nano* **2008**, *2*, 271–280.
- [28] Y. Cui, Q. Wei, H. Park, C. M. Lieber, *Science* **2001**, *293*, 1289–1292.
-